Extraction of geometrical structure of ethylene molecules by laser-induced electron diffraction combined with *ab initio* scattering calculations

Yuta Ito,[1] Richard Carranza,[2] Misaki Okunishi,[1] Robert R. Lucchese,[2] and Kiyoshi Ueda[1,*]
[1]*Institute of Multidisciplinary Research for Advanced Materials, Tohoku University, Sendai 980-8577, Japan*
[2]*Department of Chemistry, Texas A&M University, College Station, Texas 77843-3255, USA*
(Received 17 April 2017; published 15 November 2017)

We measured angle-resolved high-energy electron spectra emitted from C_2H_4 in an intense laser field, extracted field-free electron-ion elastic scattering differential cross sections (DCSs) according to quantitative rescattering theory, and obtained molecular contrast factors (MCFs) subtracting the incoherent sum of DCSs of all the atoms in the molecule. Comparing the results with *ab initio* scattering calculations and employing least-squares fitting, we have extracted the C-C and C-H bond lengths of the molecule with ∼5% uncertainty. This approach opens the way to retrieve the structure of hydrocarbon molecules, potentially at high temporal resolution, employing low collision energies where electron scattering is sensitive to the hydrogen atoms; and where the independent atom model calculations may fail to reproduce the experimentally extracted MCF.

DOI: 10.1103/PhysRevA.96.053414

I. INTRODUCTION

X-ray diffraction (XRD) and electron diffraction (ED) are well established techniques used for probing the structure of matter, in particular, the positions of atoms inside a molecule [1,2]. Recent developments of ultrafast x-ray and electron sources have opened up new possibilities for extending structure determination to the femtosecond timescale [3–5], at which atomic motion and structural changes can be investigated (see, e.g., a recent review by R. J. D. Miller [6]). Probing structural changes in gas-phase molecules at the femtosecond timescale by ED [7–9] and XRD [10–12] is still very challenging, requiring large-scale facilities and higher detection sensitivities. More importantly, ED and XRD are rather insensitive to the locations of hydrogen atoms.

The time-resolved ED described above employs external pulsed electron sources. An alternative approach for electron diffraction that uses the target's own electrons is laser-induced electron diffraction (LIED). Here a quasifree electron wave packet generated by strong laser field ionization is driven back to the parent molecular ion by the laser field and then rescattered. LIED probes the target molecular structure by measuring the rescattering photoelectrons. The concept of LIED was conceived earlier [13], and subsequently Meckel *et al.* [14] reported the pioneering experiment. To put LIED on a firm theoretical foundation, however, the development of quantitative rescattering (QRS) theory [15–17] was needed. First, extraction of laser-free elastic scattering differential cross sections (DCSs) from high-energy photoelectron spectra was proposed theoretically [15] and then proof-of-principle experiments were reported for atoms [18,19] and molecules [20,21].

In standard ED, tens to hundreds of keV electrons are used. At such high energies, the collision theory is simplified and the retrieval of bond lengths in ED relies on the independent atom model (IAM), which can be regarded as a straightforward extension of the Born approximation to scattering from molecular potentials. Using the IAM, atomic separations can be retrieved through the equivalent of the inverse Fourier transformation. However, it is not realistic to generate rescattering electrons at tens of keV or higher. On the other hand, at higher energy it is not the scattering energy that is important for scattering cross sections but the momentum transfer given by $s = 2k\sin(\theta/2)$, where k is the momentum of the electron and θ is the scattering angle. For conventional ED, the diffraction images are taken in the forward directions. For LIED, the backscattered electrons can be observed with energies on the order of a few hundred eV's, where the range of momentum transfer is similar to that of the conventional ED. In a study by Xu *et al.* [22], it was demonstrated that the DCS for a few small molecules at large scattering angles can be accurately calculated using the IAM in 100–200 eV region. Thus, the feasibility of using LIED based on the IAM to determine molecular structure was established theoretically. To apply IAM to LIED, the returning electron energy has to be larger than 100 eV for typical molecules containing C, N, and O atoms.

The first quantitative LIED experiment based on the QRS theory and IAM was carried out by Blaga *et al.* [23]. Using a ∼2-μm infrared laser, they were able to achieve 5-pm resolution for the bond lengths of N_2 and O_2. Pullen *et al.* [24] applied LIED to the laser aligned linear molecule, C_2H_2. More recently, the same group succeeded in taking a snapshot of C_2H_2, during the dissociation of the double ion leading to $C_2H^+ + H^+$ combining LIED, laser alignment, and photoelectron-photoion coincidence measurements [25]. Structural retrieval of a more complex planar molecule C_6H_6 (benzene) was also reported [26].

Furthermore, the bond lengths of not only C-C but also C-H were extracted for C_2H_2 and C_6H_6 because of sufficiently large DCSs of the H atom compared to those of the C atom at collision energies of ∼50 eV. When the energy is larger than 100 eV, the contribution from the H atom becomes small. This is an important characteristic of the LIED technique with low-energy collisions, since generally it cannot be achieved by conventional XRD and ED. In spite of such low-energy collisions, IAM has been used for structural retrieval [24–26], although the validity of the IAM has not been confirmed in this energy region. Thus, it is desirable to examine electron-ion DCSs beyond the IAM so that relatively low-energy electrons

*ueda@tagen.tohoku.ac.jp

can be considered allowing for more reliable structural retrieval for molecules containing H atoms. This can make LIED a more general technique for a variety of molecules.

In the present study, we measured photoelectron angular distributions (PADs) of C_2H_4 (ethylene) induced by an intense infrared laser. We also carried out *ab initio* electron-$C_2H_4^+$ scattering calculations, together with IAM calculations, considering the dependence on geometry. Using these results, we demonstrate that structural retrieval of hydrocarbon molecules is really possible using this approach with *ab initio* scattering calculations at collision energies less than 100 eV, where IAM calculation may fail to reproduce the DCS.

II. EXPERIMENTAL SETUP

The experimental setup is almost the same as our previous work [26]. Regeneratively amplified Ti:Sapphire laser pulses (800 nm, 100 fs, 1.5 mJ/pulse, 1 kHz) were conveyed, for pump pulses, to an optical parametric amplifier, whose output at 1650 nm was used as a driving laser for electron rescattering. The laser pulses were focused by a concave mirror (f = 75 mm) on the sample gas, which was effusively introduced and randomly oriented inside an ultrahigh vacuum chamber. The working pressure of the chamber was around 10^{-6} Torr. The momentum of electrons was measured by a field-free time-of-flight electron spectrometer with a 264-mm-length drift tube. The electrons were detected by a 40-mm-diameter microchannel plate. To obtain the angular distribution of the electrons with respect to the laser polarization direction, an achromatic half-wave plate placed in the laser path was continuously rotated once per minute for hundreds of rotations to change the polarization direction. In this way we avoided unwanted effects coming from fluctuation of the laser and increased the quality of the angular distributions obtained.

III. RESULTS AND DISCUSSION

Our theoretical approach is based on the QRS theory [16,17], in which the PAD for high-energy (rescattering) electrons is represented as a product of the returning electron wave packet and laser-free electron-parent ion elastic scattering DCS. The formulation is almost the same as our previous study [21]. In essence, this model can be thought of as an extension of the well-known three-step model. In this model, (i) the outermost electron in the molecule is first tunnel ionized at $t = t_0$; (ii) the released electron moves in the laser electric field, and, depending on the timing t_0 of the ionization in the electric fields, the electron may return to the parent ion; and (iii) the electron is scattered by the ion core elastically (or inelastically), or recombined with the molecular ion to generate high-energy photons (known as high-harmonic generation) at $t = t_r$. If the electrons are scattered at large angles, the rescattering electron will be accelerated by gaining the drift momentum A_r from the electric field during the pulse duration.

The recollision momentum p_r and the ratio of p_r to A_r are determined by the time of the ionization (t_0) and can be calculated by solving the classical equation of motion of an electron in an oscillating electric field. Electrons in trajectories that create a cutoff in the spectrum, where p_r becomes nearly

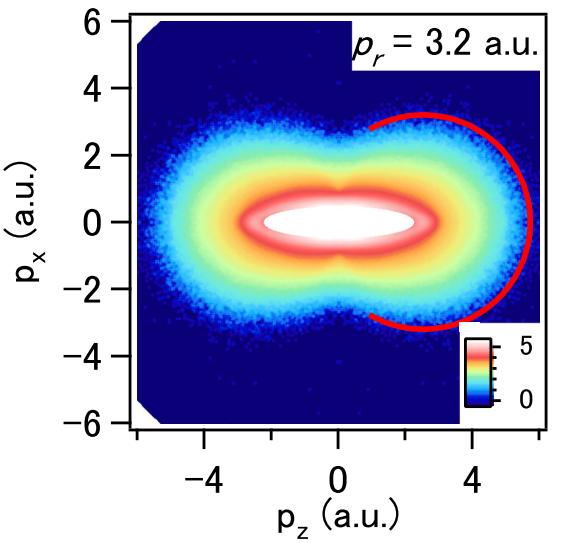

FIG. 1. A PAD of C_2H_4 measured in a 1650-nm laser field. The red circle corresponds to the rescattering electrons with a collision momentum of 3.2 a.u.

a maximum, give a p_r/A_r value of 1.26; and electrons in the long trajectories give smaller p_r and p_r/A_r values. In previous experimental studies, for example, Okunishi *et al.* [18] used a p_r/A_r value of 1.26 near the cutoff of the spectrum, and Blaga *et al.* [23] used specific p_r/A_r values for each long trajectory in the inner region of the spectrum. In the present study, we only took long trajectories having smaller p_r values than the cutoff to see the electrons located in the inner region of the spectrum.

The distribution of elastically scattered electrons at $t = t_r$ corresponds to the DCSs of electron scattering by the parent molecular ion. Only large-angle scattering with high-kinetic energy electrons are used to obtain molecular structure information. The small angle rescattering electron loses its momentum in the field. Their momentum spectra overlap and interfere with direct ionized electrons. It is difficult to extract bond lengths from such interference spectra since forward-scattered electrons, unlike back-scattered electrons, do not come close to the atomic nucleus. Even though we use a 100-fs laser pulse, we can derive the molecular geometry close to that of the neutral molecule just before the ionization, since the rescattering process completes within one optical cycle of the laser pulse (∼5 fs at the present wavelength).

A recorded PAD is shown in Fig. 1, where the laser intensity was set at 1.7×10^{14} W/cm^2. The horizontal axis (p_z) is the momentum component parallel to the laser polarization direction. Electrons having the maximum p_r of ∼3.2 a.u. are observed, whose corresponding energy is 139 eV. Because there are fewer electron counts at the outermost part of the spectrum, we took electrons located at the inner part (small p_r), dominated by the long trajectories as mentioned above, for further analysis.

DCSs were extracted from experimental results according to QRS theory as shown in Fig. 2. In the IAM, the DCS of electron-molecule scattering (σ) is approximated by the sum

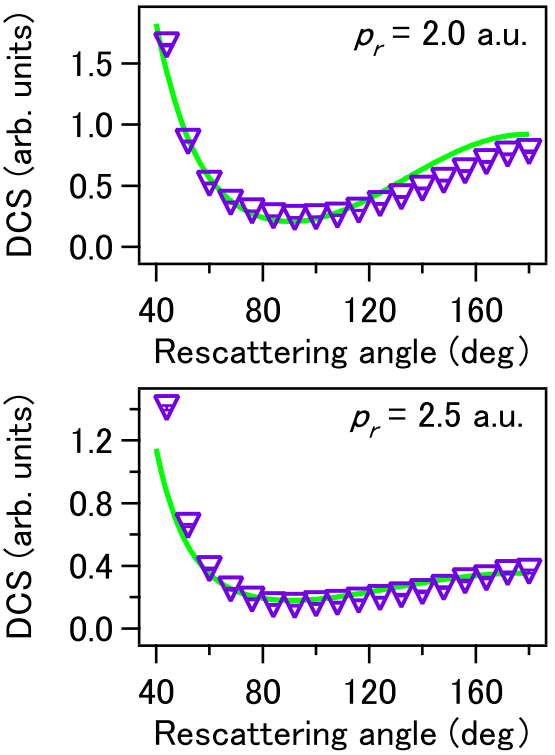

FIG. 2. DCSs of field-free electron-ion elastic scattering extracted from the spectrum shown in Fig. 1 for $p_r = 2.0$ a.u. and 2.5 a.u. The (green) solid line is the sum of theoretical atomic DCSs.

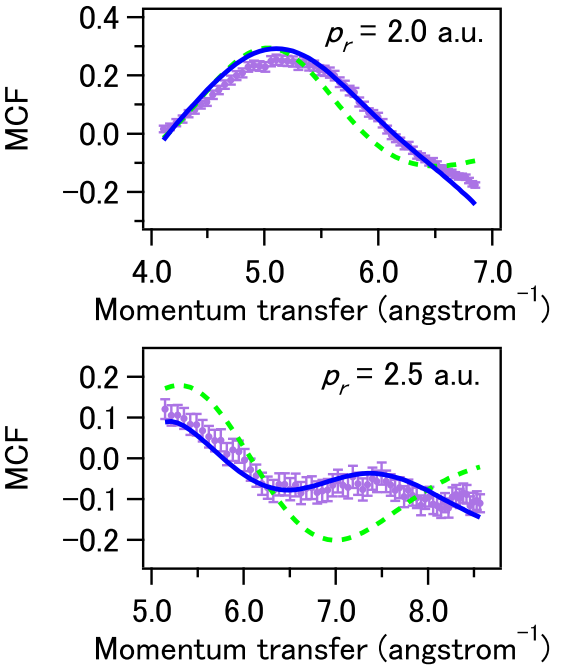

FIG. 3. MCFs derived from the experimental DCSs shown in Fig. 2. Theoretical MCFs are also shown for e^--$C_2H_4^+$ scattering (blue solid line) and IAM (green dashed line).

of atomic terms and molecular interference terms,

$$\sigma = \sum_i |f_i|^2 + \sum_{i \neq j} f_i f_j^* e^{-isr_{ij}}, \quad (1)$$

where f_i is the atomic scattering factor, $s = 2p_r \sin\theta_r/2$ is the momentum transfer, and r_{ij} is the interatomic distance. Theoretically calculated atomic scattering factors are available in a database [27,28]. Atomic DCS (σ_A), the first term on the right-hand side of Eq. (1), is the sum of DCSs of electron-atom scattering for each atom constituting the molecule, containing no information on the molecular geometry. The molecular interference term (the second term) comes from interference of scattering amplitudes between every pair of atoms in the molecule, reflecting the interatomic distances. In gas-phase ED, the interference term is observed as a small deviation from the atomic DCS. Therefore, the atomic DCS is a good indicator of the quality of the experimentally extracted DCSs. In Fig. 2, a sum of theoretical atomic DCSs is shown as the green line. The experimental and atomic DCSs exhibit very similar trends for each p_r, indicating that the signal comes from elastic scattering between an electron and the C_2H_4 molecule. Furthermore, it suggests that extraction of the DCSs from the experimental data has been done correctly.

The molecular contrast factor (MCF) is defined as

$$\text{MCF} = \frac{\sigma - \sigma_A}{\sigma_A}, \quad (2)$$

and is helpful for extracting information about the molecular geometry. In Eq. (2), σ is an experimental or theoretical molecular DCS and σ_A is the sum of theoretical atomic DCSs, i.e., the first sum on the right hand side of Eq. (1). Experimental MCFs are given in Fig. 3 as a function of the momentum transfer. They show clear oscillatory structure, indicating that the information about the molecular structure is captured in the MCFs.

In the present study we compare experimental with theoretical MCFs. The theoretical calculations for the field free DCSs of electron scattering from $C_2H_4^+$ were based on a Hartree-Fock (HF) description of C_2H_4. The orbitals for the ion state were taken to be the same as for the neutral HF state, which were obtained with the augmented correlation-consistent polarized valence triple-ζ (aug-cc-pVTZ) one-electron basis set using the GAUSSIAN program [29]. Using the fixed-nuclei approximation, the scattering matrices in the molecular frame at a series of geometries were computed using the Schwinger variational method within the EPOLYSCAT suite of programs [30,31]. An $l_{\max} = 60$ was used for the single-center expansion of the electronic wave functions, and the electron-molecule interaction potential was the static-exchange with model polarization (SEP), where electron polarization effects in the scattering dynamics are included using the Perdew-Zunger correlation potential [32]. Next, a weighted average over orientations of the molecule relative to the field polarization was taken using the angle-dependent ionization probability, which was calculated with weak-field asymptotic theory [33,34] and used in our previous study [21]. Finally, MCFs were obtained using Eq. (2) with the orientation averaged DCSs. In Fig. 3, theoretical MCFs are also plotted for e^--$C_2H_4^+$ SEP calculations in the blue solid line. The theoretical calculations reproduce the experimental results quite well for both p_r. Theoretical results with IAM are shown in the green dashed line. The IAM results are fairly close to the experimental data for $p_r = 2.0$ a.u. However,

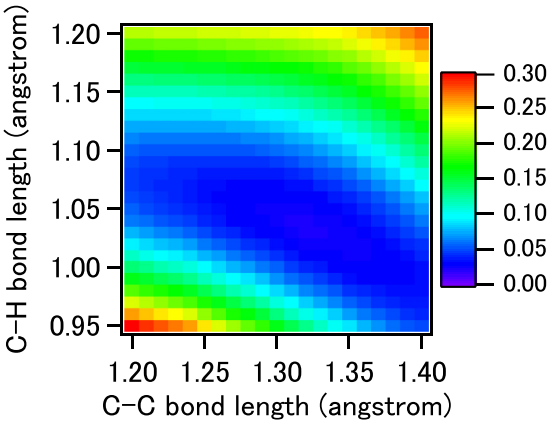

FIG. 4. Residual sum of squares between the experimental and theoretical MCFs for $p_r = 2.5$ a.u. as a function of the bond lengths.

for $p_r = 2.5$ a.u. there are significant differences between the IAM and experimental MCFs. For these p_r, the residual sum of squares of the difference between the MCF from the SEP calculation and the experiment was a factor of 5–10 better than that obtained from the IAM calculation. These differences are particularly pronounced for momentum transfers above 6.5 $Å^{-1}$.

The differences clearly show the limitations of the IAM in the present momentum range. Multiple scattering and nonspherical electron densities, which are included in the SEP scattering calculations but are neglected in the IAM, are sources of errors in the IAM. Thus, the extracted MCFs from the experimental and theoretical DCSs by using Eq. (2) indicate the interference effects, although the failure of the IAM implies that the MCF cannot be easily interpreted, i.e., it does not simply correspond to the interference term found in Eq. (1).

Finally, using the SEP approximation, we calculated MCFs by changing the C=C and C-H bond lengths and keeping the bond angles fixed. We then obtained the residual sum of squares between the experimental and theoretical MCFs. The result for $p_r = 2.5$ a.u. is shown in Fig. 4. A clear minimum can be seen, indicating that the theoretical MCF reflects the molecular geometry, although it involves complicated structure beyond IAM. By finding the minimum value of the residual sum of squares, we determined bond lengths from the present experimental data. We found C=C and C-H bond lengths of 1.28(5) Å and 1.15(3) Å at $p_r = 2.0$ a.u. and 1.32(9) Å and 1.04(7) Å at $p_r = 2.5$ a.u. The results are very close to the equilibrium geometry of the neutral species, 1.34 Å and 1.09 Å for C=C and C-H with ∼5% difference. We have estimated the statistical uncertainty in bond lengths numerically where the parameters are on the boundary of the 95% confidence region [35]. It should be noted that the bond lengths given by the *ab initio* approach strongly rely on the accuracy of the calculated DCSs, where the interpretation of the interference pattern is relatively indirect compared with conventional ED using Fourier transform at high collision energy. A similar extraction of the geometry using the IAM MCF calculations again led to a significantly worse optimum fit with $p_r = 2.0$ a.u. and did not find a well defined best fit in the case of $p_r = 2.5$ a.u.

IV. CONCLUSION

In summary, we measured the PADs induced by a 1650-nm intense laser field, extracted DCSs of field-free electron-$C_2H_4^+$ elastic scattering, and derived MCFs from them. To obtain the C-H and C-C bond lengths from the experimental MCFs, we employed *ab initio* calculations with the SEP approximation, instead of the commonly used IAM. The agreement of the experimental MCFs with the *ab initio* results are significantly better than that with the IAM results, illustrating that the *ab initio* approach is superior to the IAM. As a consequence, the present fitting approach achieved a 5% deviation from experiment with 95% confidence for the results of the bond length extractions. As demonstrated here, LIED combined with the *ab initio* calculations improves its reliability for its application to hydrogen-containing molecules, such as hydrocarbons, where proper treatment of low-energy scattering is essential for the method to be sensitive to hydrogen atoms.

ACKNOWLEDGMENTS

This work was supported in part by grants-in-aid for scientific research from JSPS Grant No. JP17K05739, by the X-Ray Free Electron Laser Utilization Research Project and the X-Ray Free Electron Laser Priority Strategy Program of the Ministry of Education, Culture, Sports, Science and Technology of Japan, Dynamic Alliance for Open Innovation Bridging Human, Environment and Materials, and IMRAM research program. The work at Texas A&M University was supported by the United States Department of Energy, Office of Science, Basic Energy Science, Geoscience, and Biological Divisions, under Award No. DE-SC0012198. R.C. was supported by the Robert A. Welch Foundation (Houston, Texas) under Grant No. A-1020. Also, the assistance and computer time provided by the Supercomputing Facility at Texas A&M University are acknowledged. We also thank Professor T. Morishita for providing us the angle-dependent ionization rates of C_2H_4.

[1] E. Wollan, Rev. Mod. Phys. **4**, 205 (1932).
[2] L. Brockway, Rev. Mod. Phys. **8**, 231 (1936).
[3] J. Tenboer, S. Basu, N. Zatsepin, K. Pande, D. Milathianaki, M. Frank, M. Hunter, S. Boutet, G. J. Williams, J. E. Koglin *et al.*, Science **346**, 1242 (2014).
[4] T. R. M. Barends, L. Foucar, A. Ardevol, K. Nass, A. Aquila, S. Botha, R. B. Doak, K. Falahati, E. Hartmann, M. Hilpert *et al.*, Science **350**, 445 (2015).
[5] K. R. Ferguson, M. Bucher, T. Gorkhover, S. Boutet, H. Fukuzawa, J. E. Koglin, Y. Kumagai, A. Lutman, A. Marinelli, M. Messerschmidt *et al.*, Sci. Adv. **2**, e1500837 (2016).

[6] R. J. D. Miller, Science **343**, 1108 (2014).
[7] A. H. Zewail and H. Z. Ahmed, *4D Visualization of Matter* (World Scientific, Singapore, 2014).
[8] C. J. Hensley, J. Yang, and M. Centurion, Phys. Rev. Lett. **109**, 133202 (2012).
[9] J. Yang, M. Guehr, X. Shen, R. Li, T. Vecchione, R. Coffee, J. Corbett, A. Fry, N. Hartmann, C. Hast *et al.*, Phys. Rev. Lett. **117**, 153002 (2016).
[10] J. Küpper, S. Stern, L. Holmegaard, F. Filsinger, A. Rouzée, A. Rudenko, P. Johnsson, A. V. Martin, M. Adolph, A. Aquila *et al.*, Phys. Rev. Lett. **112**, 083002 (2014).
[11] M. P. Minitti, J. M. Budarz, A. Kirrander, J. S. Robinson, D. Ratner, T. J. Lane, D. Zhu, J. M. Glownia, M. Kozina, H. T. Lemke *et al.*, Phys. Rev. Lett. **114**, 255501 (2015).
[12] J. M. Glownia, A. Natan, J. P. Cryan, R. Hartsock, M. Kozina, M. P. Minitti, S. Nelson, J. Robinson, T. Sato, T. van Driel *et al.*, Phys. Rev. Lett. **117**, 153003 (2016).
[13] T. Zuo, A. D. Bandrauk, and P. B. Corkum, Chem. Phys. Lett. **259**, 313 (1996).
[14] M. Meckel, D. Comtois, D. Zeidler, A. Staudte, D. Pavičić, H. C. Bandulet, H. Pépin, J. C. Kieffer, R. Dörner, D. M. Villeneuve *et al.*, Science **320**, 1478 (2008).
[15] T. Morishita, A.-T. Le, Z. Chen, and C. D. Lin, Phys. Rev. Lett. **100**, 013903 (2008).
[16] Z. Chen, A.-T. Le, T. Morishita, and C. D. Lin, J. Phys. B **42**, 061001 (2009).
[17] C. D. Lin, A.-T. Le, Z. Chen, T. Morishita, and R. Lucchese, J. Phys. B **43**, 122001 (2010).
[18] M. Okunishi, T. Morishita, G. Prümper, K. Shimada, C. D. Lin, S. Watanabe, and K. Ueda, Phys. Rev. Lett. **100**, 143001 (2008).
[19] D. Ray, B. Ulrich, I. Bocharova, C. Maharjan, P. Ranitovic, B. Gramkow, M. Magrakvelidze, S. De, I. V. Litvinyuk, A.-T. Le *et al.*, Phys. Rev. Lett. **100**, 143002 (2008).
[20] M. Okunishi, H. Niikura, R. R. Lucchese, T. Morishita, and K. Ueda, Phys. Rev. Lett. **106**, 063001 (2011).
[21] C. Wang, M. Okunishi, R. R. Lucchese, T. Morishita, O. I. Tolstikhin, L. B. Madsen, K. Shimada, D. Ding, and K. Ueda, J. Phys. B **45**, 131001 (2012).
[22] J. Xu, Z. Chen, A.-T. Le, and C. D. Lin, Phys. Rev. A **82**, 033403 (2010).
[23] C. I. Blaga, J. Xu, A. D. Di., E. Sistrunk, K. Zhang, P. Agostini, T. A. Miller, L. F. DiMauro, and C. D. Lin, Nature **483**, 194 (2012).
[24] M. G. Pullen, B. Wolter, A.-T. Le, M. Baudisch, M. Hemmer, A. Senftleben, C. D. Schröter, J. Ullrich, R. Moshammer, C. D. Lin *et al.*, Nat. Commun. **6**, 7262 (2015).
[25] B. Wolter, M. G. Pullen, A. T. Le, M. Baudisch, K. Doblhoff-Dier, A. Senftleben, M. Hemmer, C. D. Schroeter, J. Ullrich, T. Pfeifer *et al.*, Science **354**, 308 (2016).
[26] Y. Ito, C. Wang, A.-T. Le, M. Okunishi, D. Ding, C. D. Lin, and K. Ueda, Struct. Dynam. **3**, 034303 (2016).
[27] NIST Electron Elastic-scattering Cross-section Database: Version 3.2, NIST Standard Reference Database No. 64.
[28] F. Salvat, A. Jablonski, and C. Powell, Comput. Phys. Commun. **165**, 157 (2005).
[29] M. J. Frisch, G. W. Trucks, H. B. Schlegel, G. E. Scuseria, M. A. Robb, J. R. Cheeseman, G. Scalmani, V. Barone, G. A. Petersson, H. Nakatsuji *et al.*, *Gaussian 16 Revision A.03* (Gaussian Inc., Wallingford, CT, 2016).
[30] F. Gianturco and R. Lucchese, J. Chem. Phys. **108**, 6144 (1998).
[31] F. Gianturco, R. Lucchese, and N. Sanna, J. Chem. Phys. **102**, 5743 (1995).
[32] J. P. Perdew and A. Zunger, Phys. Rev. B **23**, 5048 (1981).
[33] O. I. Tolstikhin, T. Morishita, and L. B. Madsen, Phys. Rev. A **84**, 053423 (2011).
[34] L. B. Madsen, O. I. Tolstikhin, and T. Morishita, Phys. Rev. A **85**, 053404 (2012).
[35] W. H. Press, S. Teukolsky, W. Vetterling, and B. Flannery, *Numerical Recipes in C: The Art of Scientific Computing*, 2nd ed. (Cambridge University Press, New York, 1992).